

EMISSION FROM NONRELATIVISTIC ELECTRONS IN THIN METAL FOILS

F. R. ARUTYUNYAN, Zh. V. PETROSYAN, and R. A. OGANESYAN

Joint Radiation Laboratory, Academy of Sciences, Armenian S.S.R. and Erevan Physics Institute,
Erevan State University

Submitted to JETP editor April 8, 1966

J. Exptl. Theoret. Phys. (U.S.S.R.) 51, 760-772 (September, 1966)

Optical radiation ($\lambda = 3480\text{--}5500 \text{ \AA}$) emitted when 60-keV electrons having energies up to 60 keV traverse thin ($d = 200\text{--}1340 \text{ \AA}$) silver and gold foils is investigated experimentally. The spectral and angular distributions of the radiation and the dependence of its intensity on electron energy and film thickness are investigated for photons polarized in the plane containing the normal to the foil surface and the direction of observation (the emission plane) and in the perpendicular plane. The properties of the light polarized in the emission plane agree completely with the Ginzburg-Frank theory of transition radiation. Light polarized in the perpendicular plane is identified as bremsstrahlung. The polarization of the radiation is also analyzed.

1. INTRODUCTION

WHEN a charged particle crosses the interface of two media having different optical properties transition radiation is emitted, as was predicted by Ginzburg and Frank in 1945.^[1,2] This radiation results from changes in the electromagnetic field moving with the particle, either because of a change in the velocity of wave propagation, or as a result of light absorption by one of the media. Transition radiation is characterized by complete polarization in the emission plane, which is the plane containing the direction of photon propagation and a normal to the interface. The theory of this effect was subsequently developed in numerous articles, which are reviewed in detail in^[3-6].

The transition radiation from a charged particle traversing a thin layer of matter was first studied by Pafomov,^[7] and later by the authors of^[8-10]. In this case the transition radiation intensity depends on the thickness of the layer and is exhibited most clearly with transparent films, where there is interference between the radiation from both faces.

The enhanced interest in transition radiation has obviously resulted from the possibilities of utilizing this radiation to determine the optical constants of metals, to generate electromagnetic waves in the millimeter region,^[11] to detect particles having ultrahigh energies^[12] etc.

The experimental investigations of transition radiation properties during the past few years^[13-18] have confirmed the fundamental theory. The experiments have been analyzed in^[6,9]. However,

additional experimental work is needed to achieve more complete and detailed knowledge of the properties of transition radiation and for practical applications.

We have investigated the properties of radiation generated in aluminum, gold, and silver foils traversed by 60-keV electrons. We have previously^[19,20] analyzed the experimental results for aluminum and gold foils. In the present work we discuss the results obtained with silver and gold foils. The experimental data are compared with the transition-radiation formula for a foil^[7] and with the formulas for bremsstrahlung.^[17,21]

2. EXPERIMENT

The radiation generated during the passage of charged particles through metal foils was investigated with electrons having energies up to 60 keV. The experimental scheme is shown in Fig. 1. The electron source was a Pierce-type electron gun that supplied a continuous parallel electron beam of 0.5-cm diameter in currents up to 1 mA. An electromagnet deflected the electron beam 45° from its initial direction. A thin magnetic lens focused the beam at the center of the target (emission) chamber containing the investigated foils. Deflection of the beam was required to prevent the entrance of light from the glowing cathode of the gun into the target chamber and its subsequent detection.

The electron beam produced a luminous spot 0.1 cm in diameter on the target. The impinging

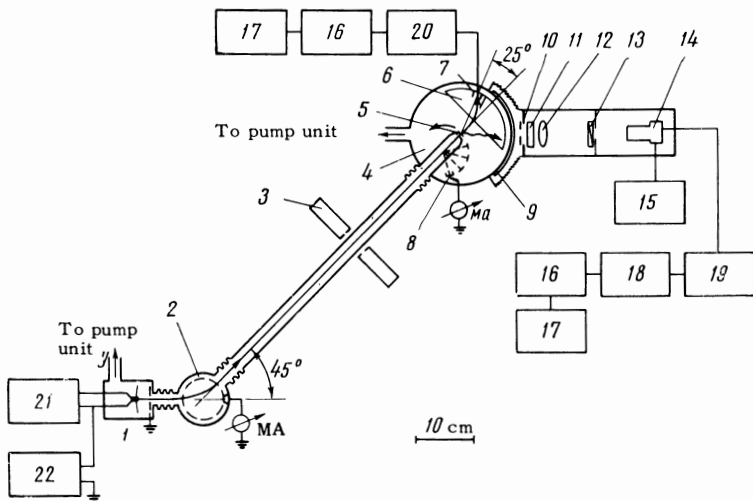


FIG. 1. Experimental scheme. 1 – electron gun, 2 – magnet pole, 3 – magnetic lens, 4 – target chamber, 5 – target, 6 – magnet pole tip, 7 – main Faraday cup, 8 – auxiliary Faraday cup, 9 – transparent window, 10 – diaphragm (14-mm diameter), 11 – interference filter, 12 – quartz lens ($F = 110$ mm), 13 – polarizing filter, 14 – FEU-17A photomultiplier, 15 – photomultiplier power supply, 16 – integrating device, 17 – measuring device, 18 – millimicroammeter, 19 – compensator of photomultiplier dark current, 20 – microammeter, 21 – power supply of electron gun filament, 22 – high-voltage power supply of electron gun.

beam current was maintained at an average of $1\text{--}2\ \mu\text{A}$. More intense beams cause wrinkling of the foil; this effect is enhanced with increasing beam current and occurs in thick foils at relatively low current levels. Secondly, in the case of high currents the properties of the foil change even during the time required to measure any feature of the radiation.

For the purpose of studying small-angle emission, the electron beam, after traversing the target (in the target chamber) was deflected 25° by a magnetic field and entered the main Faraday cup. To prevent the stray field of the magnet from affecting the beam focusing on the target, the electron duct before the target in the target chamber was made of magnetic material and terminated in a collimator of 0.08-cm aperture. The beam divergence at the target was $\pm 3^\circ$.

The system was evacuated at the electron gun and the target chamber, where pressures of $(2\text{--}4) \times 10^{-6}$ and $(1\text{--}2) \times 10^{-5}$ mm Hg, respectively, were maintained. A semiconductor vacuum trap located between the diffusion pump and the target chamber prevented oil vapor from entering the chamber and condensing on the target.

The entire system was coated internally with Aquadag to reduce electron scattering and bremsstrahlung in the target chamber and to absorb stray light. Aquadag was also used to coat all the aluminum Faraday cups measuring the beam current. The target chamber was able to hold simultaneously four different targets and the auxiliary Faraday cup, all of which were suspended from radial metal rods attached to a common vertical axis. The targets and the Faraday cup were transferred into the path of the beam in the center of the chamber by rotation of this axis, without affecting the vacuum.

Each target was an aluminum ring of 1-cm diameter, on which there was first deposited a thin

plastic film as a backing, followed by a vacuum-deposited metal layer of the required thickness. Silver, aluminum, and gold foils were deposited at the rate of 50, 200, and $30\ \text{\AA}/\text{min}$, respectively, under $\sim 10^{-4}$ mm pressure. The foil thicknesses were measured by optical interferometry to within $\pm 10\ \text{\AA}$.

The investigated emission was observed through an optically polished transparent plastic window located in the side wall of the target chamber within the angular region $0\text{--}90^\circ$. Light emitted at any given angle θ within a solid angle of 4.09×10^{-3} sr defined by a diaphragm, was focused by a quartz lens ($F = 110$ mm) on the photocathode of an FEU-17 photomultiplier. The spectral characteristics of the emission at wavelengths from 3480 to $5500\ \text{\AA}$ were investigated with interference filters, while its polarization was investigated with a polarization filter capable of 360° rotation around the optical axis of the system.

In the absence of a standard light source for calibration of the detecting system, we calculated the efficiency of the latter. The transmission of each separate optical element (lens, polarizing filter, chamber window) was measured with an SF-4 spectrophotometer. The nominal ratings were used for the transmission at the maximum and for the band widths of the interference filters, for the spectral sensitivity and quantum yield of the photocathode at maximum spectral sensitivity, and for the photomultiplier amplification. The detection efficiency of the system determined in this manner can obviously deviate from its true value, and can therefore lead to some underestimation or overestimation of the absolute radiation intensities.

The photomultiplier output was fed to an integrator. A sensitive EMU-3 vacuum-tube millivoltmeter measured the potential built up on the condenser during determinate time intervals. The

potential generated during the same time interval by the electron beam current reaching the main Faraday cup was measured similarly at the same time. Because of electron scattering in the target not all electrons producing radiation will strike the main Faraday cup. Therefore the currents to the main and auxiliary Faraday cups were measured, yielding a ratio from which the true number of radiating electrons can be derived.

The angular and polarizing properties of the optical system were tested. The target was replaced by a vertical 0.1-cm diameter tungsten filament heated by an electric current and emitting unpolarized isotropic light. A horizontal gap 0.1 cm wide was positioned in front of the filament. Detection of the light at different angles and for different transmitting directions of the polarizing filter showed that the system possessed no intrinsic angular or polarizing properties.

We also measured the radiation produced in the target chamber when the operating electron beam traversed only the backing of the foil. The result fell within the fluctuation limits of a dark current averaging $\pm 2 \times 10^{-9}$ A.

Preceding each measurement the photomultiplier dark current, which was 10^{-8} A at 1250-V operating voltage, was compensated by a suitable device and its fluctuations were determined. Each final result was the average of three measurements.

3. EXPERIMENTAL RESULTS AND DISCUSSION

We investigated the radiation originating in silver and gold foils from 202 to 1341 Å thick traversed by electrons up to 60 keV. The radiation was partly polarized with the sign predicted by the theory of transition radiation. The degree of polarization increased with electron energy and reached a maximum of $\sim 85\%$ at observation angles $\theta = 50\text{--}60^\circ$ for $E = 60$ keV.

Light polarized in the emission plane and perpendicular thereto will henceforth be designated as the parallel and perpendicular radiation components, respectively. The degree of polarization for silver foils was smaller than for aluminum ($\sim 98\%$ ^[19]) and gold ($\sim 89\%$ ^[20]) foils because of the larger perpendicular component associated with the silver foils.

The intensity of the unpolarized portion of the radiation was taken as equal to the observed perpendicular component, and the theory of transition radiation was compared with the intensity difference between the parallel and perpendicular components. Temporarily disregarding the nature of the perpendicular light, we note that its intensity is

much lower than that of the parallel component. Therefore the foregoing comparison is all the more fully justified, because the indicated difference, as will be seen, yields the typical properties of transition radiation.

a) Transition radiation. The solid curves in the figures that follow correspond to the theory of transition radiation.^[7] The optical constants of silver foils were taken from^[22].

A comparison with experiment showed that the absolute intensity of the observed radiation exceeds its theoretical value by the factor 1.5. It appears, as we have mentioned in^[19,20], that this deviation is associated with uncertainty in our knowledge of the detection system efficiency. This argument is strengthened by the fact that the experimental results exceed the theory by an equal factor (within 15%) for aluminum, gold, and silver foils. In comparison with the theory the experimental results will henceforth be given with values reduced by the factor 1.5.

The dependence of the radiation intensity on electron energy from 30 to 60 keV is shown in Fig. 2. Independently of the emitted wavelength, the angle of observation, and the silver foil thickness, the experimental results exhibit a linear growth of brightness with electron energy, in good agreement with the theory.

The spectral density observed at different angles within the $\sim 10\%$ limits of experimental errors corresponds to the expected theoretical result (Fig. 3). The investigated 3480–5500-Å wavelength interval does not include the silver transparency region, where many authors observed a characteristic peak in the region 3200–3300 Å.

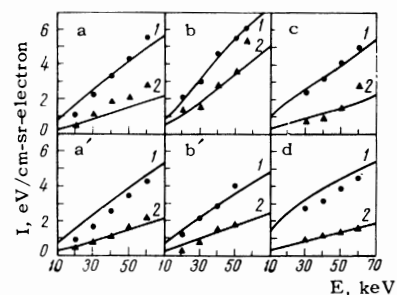


FIG. 2. Dependence of transition radiation intensity on electron energy. a - $\lambda = 5100$ Å, $d = 660$ Å: curve 1, $\bullet - \theta = 55^\circ$, curve 2, $\blacktriangle - \theta = 25^\circ$; a' - $\lambda = 5100$ Å, $d = 837$ Å: curve 1, $\bullet - \theta = 55^\circ$; 2, $\blacktriangle - \theta = 25^\circ$; b - $\lambda = 4000$ Å, $d = 767$ Å: curve 1, $\bullet - \theta = 60^\circ$, 2, $\blacktriangle - \theta = 30^\circ$; b' - $\lambda = 5500$ Å, $d = 767$ Å: curve 1, $\bullet - \theta = 60^\circ$, 2, $\blacktriangle - \theta = 30^\circ$; c - $\lambda = 3820$ Å, $d = 1341$ Å: curve 1, $\bullet - \theta = 60^\circ$, 2, $\blacktriangle - \theta = 20^\circ$; d - $\lambda = 4670$ Å, $d = 344$ Å: curve 1, $\bullet - \theta = 60^\circ$, 2, $\blacktriangle - \theta = 20^\circ$.

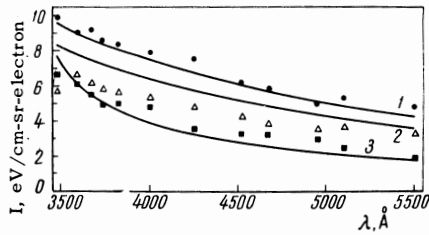


FIG. 3. Spectral distributions of transition radiation. Curve 1, \bullet - $E = 50$ keV, $\theta = 55^\circ$, $d = 662$ Å; 2, \blacktriangle - $E = 50$ keV, $\theta = 55^\circ$, $d = 662$ Å; 3, \blacksquare - $E = 50$ keV, $\theta = 30^\circ$, $d = 633$ Å.

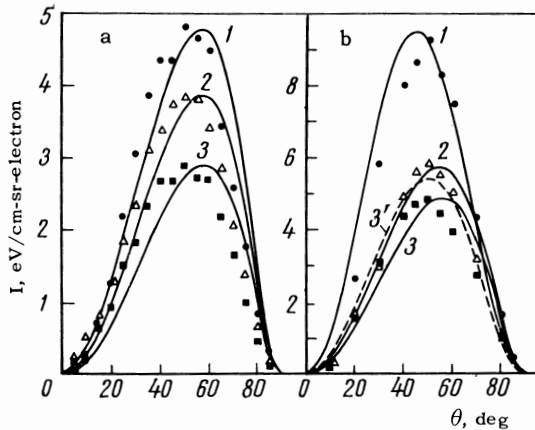


FIG. 4. Angular distribution of transition radiation. a - $\lambda = 4670$ Å, $d = 716$ Å: curve 1, \bullet - $E = 50$ keV, 2, \triangle - $E = 40$ keV, 3, \blacksquare - $E = 30$ keV; b - $d = 666$ Å, $E = 50$ keV: curve 1, \bullet - $\lambda = 3480$ Å, 2, \triangle - $\lambda = 4250$ Å, 3, \blacksquare - $\lambda = 4670$ Å; 3' - curve 3 for $\chi = 1.50$.

Figure 4 shows the angular distributions of intensities measured at different wavelengths. The data indicate a characteristic dependence of transition radiation intensity on the observation angle. Also, as can be seen from Fig. 4b, the experimental distributions are shifted relative to the corresponding theoretical curves. For short wavelengths (3480 Å) this shift is in the direction of larger angles, whereas for relatively long waves up to 5500 Å the shift is in the direction of smaller angles. We have observed similar shifts of the angular distributions for aluminum foils.^[19] The shifts are apparently associated with the fact that we used optical constants for the foils that did not agree with those for which the theoretical curves were plotted. For example, Fig. 4b shows the angular distribution of transition radiation calculated for 4670 Å with $\chi = 1.50$ (curve 3') taken for the absorption coefficient instead of 2.54 (curve 3). Curve 3' agrees better with experiment than curve 3 does. Assuming that this shift results only from a different absorption coefficient for silver, the experimental findings indicate that χ is larger for short wavelengths, and is smaller for long wavelengths, than in^[22].

On the basis of the same assumption it follows from the data for aluminum foils^[19] that χ for 3730 Å and 4670 Å has smaller values than those used in calculating the theoretical curves, whereas this is not indicated for gold foils.^[20] From Fig. 4a, showing the angular distributions measured at 4670 Å for different incident electron energies, it follows that all curves are shifted to the same degree relative to the theoretical curves. Of all transition radiation properties the angular distributions are most sensitive to variation of the optical constants for metal foils.

Transition radiation is especially distinguished by the oscillatory dependence of its intensity on foil thickness. Figure 5 shows this for silver foils with thicknesses up to 1000 Å at two different angles of observation. It must be emphasized that the comparison of theory with experiment is rendered somewhat difficult by the fact that the theoretical curves were calculated neglecting the differences of the constants for the different foil thicknesses in view of the absence of data. Nevertheless, the experimental results show the theoretically expected dependence on the thickness. The oscillatory character of this dependence affects short wavelengths most because of the relatively small absorption coefficient of silver. The oscillations are almost absent for long wavelengths and the emission is actually produced at a single boundary.

b) **Bremsstrahlung.** The investigations showed that the magnitude of the perpendicular component depends on the metal; it is negligibly small for aluminum, with which the background oscillations of the dark current are registered in actuality. For gold foils this signal exceeds the background but remains of comparable magnitude with the latter;

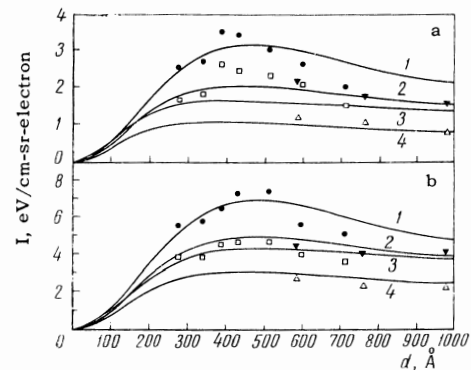


FIG. 5. Intensity of transition radiation vs foil thickness. a - $\theta = 25^\circ$, $E = 50$ keV: curve 1, \bullet - $\lambda = 4000$ Å, 2, \square - $\lambda = 4670$ Å; $\theta = 25^\circ$, $\lambda = 5500$ Å: curve 3, \blacktriangledown - $E = 60$ keV; 4, \triangle - $E = 40$ keV. b - $\theta = 50^\circ$, $E = 50$ keV: curve 1, \bullet - $\lambda = 4000$ Å, 2, \square - $\lambda = 4670$ Å; $\theta = 55^\circ$, $\lambda = 5500$ Å: curve 3, \blacktriangledown - $E = 60$ keV, 4, \triangle - $E = 40$ keV.

for silver foils it is relatively large and greatly exceeds the background in some instances.

In principle the perpendicular component can consist of bremsstrahlung, luminescence originating in the metal surface layer, and transition radiation arising from electrons scattered in the foil and leaving it at an oblique angle. The intensities of bremsstrahlung and luminescence are known to possess $1/E$ dependence on electron energy, while the perpendicular component of transition radiation exhibits E^2 dependence for oblique electron incidence.^[23] Therefore the observed radiation is divided into two parts, proportional to E^2 and $1/E$, respectively.

Figure 6 shows the dependences of the perpendicular radiation intensity on electron energy for silver and gold foils of different thicknesses for different observation angles. These curves differ from the analogous curves for the parallel component, and in most cases they exhibit decreasing intensity as the electron energy is increased. The $1/E$ and E^2 components are shown; it is seen that at low electron energies the main contribution to the total radiation comes from the $1/E$ component, while at high energies the two components are approximately equal. The absence of I_{\perp} for aluminum foils in our earlier approximation^[19] together with the data^[15] for several other metals show that the luminescence is unimportant. Therefore the $1/E$ component is compared with the corresponding bremsstrahlung component. Curves 1 in Figs. 6–9 represent the bremsstrahlung theory calculated for an isolated atom,^[21] while curves 2 represent the theory for foils when the medium is taken into account.^[17]

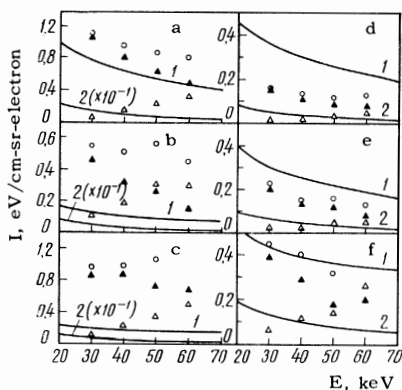


FIG. 6. Intensity of perpendicular radiation component vs electron energy. \blacktriangle – component $\sim 1/E$, \bigcirc – component $\sim E^2$, \bigcirc – total radiation. 1 – theoretical curve for bremsstrahlung, ^[21] 2 – from ^[17] (for Ag curve 2 is elevated by the factor 10). a – Ag, $\lambda = 3820 \text{ \AA}$, $d = 1341 \text{ \AA}$, $\theta = 60^\circ$; b – Ag, $\lambda = 4670 \text{ \AA}$, $d = 334 \text{ \AA}$, $\theta = 60^\circ$; c – Ag, $\lambda = 4670 \text{ \AA}$, $d = 334 \text{ \AA}$, $\theta = 20^\circ$; d – Au, $\lambda = 4670 \text{ \AA}$, $d = 361 \text{ \AA}$, $\theta = 60^\circ$; e – Au, $\lambda = 3820 \text{ \AA}$, $d = 202 \text{ \AA}$, $\theta = 60^\circ$; f – Au, $\lambda = 3820 \text{ \AA}$, $d = 202 \text{ \AA}$, $\theta = 20^\circ$.

The experimental data for gold foils show that the observed intensity lies between these curves. Since these data are comparable with the neglected experimental background, we can affirm that the results do not conflict with the theory that takes the optical constants into account. The data for silver lie high above the bremsstrahlung curve taking the medium into account, and also lie above the curve for an isolated atom. It should be noted that according to^[17] the yield of bremsstrahlung from a foil is strongly enhanced as the absorption coefficient of the material decreases, and for small values of the latter can even exceed the yield in the case of an isolated atom. However, when discussing the experimental results for transition radiation we mentioned that better agreement between theory and experiment results if it is assumed that the absorption coefficients of our silver foils are smaller than the values used in plotting the theoretical curves. The large bremsstrahlung yield from silver is apparently associated with this circumstance.

The experimental dependences of radiation intensity on electron energy for different observation angles, wavelengths, and foil thicknesses were used to decompose the angular and spectral distributions and the dependence of intensity on foil thickness into the components that are proportional to $1/E$ and E^2 .

Figure 7 shows the angular distributions of the perpendicular component for gold (Fig. 7a) and silver (Fig. 7b) foils. The $1/E$ and E^2 components for one of the silver curves, shown in Fig. 7c, reveal that the $\sim 1/E$ part has angular dependence resembling that of bremsstrahlung, while the $\sim E^2$ part has angular dependence similar to that of the

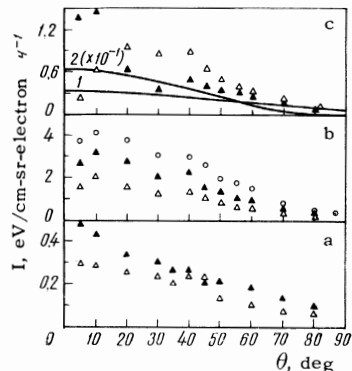


FIG. 7. Angular distributions of the perpendicular component. a – Au, $E = 60 \text{ keV}$, $d = 361 \text{ \AA}$: \blacktriangle – $\lambda = 3820 \text{ \AA}$, \bigcirc – $\lambda = 4670 \text{ \AA}$. b – Ag, $E = 50 \text{ keV}$, $d = 666 \text{ \AA}$: \bigcirc – $\lambda = 3480 \text{ \AA}$, \blacktriangle – $\lambda = 4250 \text{ \AA}$, \triangle – $\lambda = 4670 \text{ \AA}$. c – Ag, $E = 50 \text{ keV}$, $d = 666 \text{ \AA}$, $\lambda = 4670 \text{ \AA}$: \blacktriangle – $\sim 1/E$ component; \triangle – $\sim E^2$ component; curve 1 – theoretical for bremsstrahlung from ^[21], 2 – from ^[17] (enhanced 10 times).

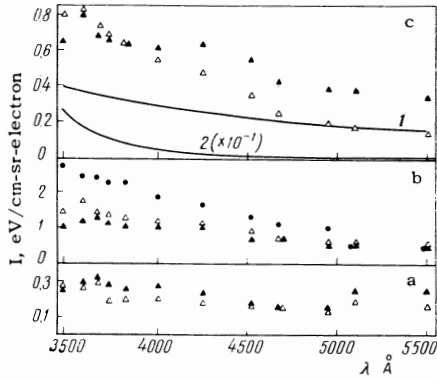


FIG. 8. Spectral distributions of the perpendicular component. a – Au, $E = 60$ keV, $d = 327$ Å: \blacktriangle – $\theta = 30^\circ$, \triangle – $\theta = 50^\circ$. b – Ag, $d = 662$ Å, $\theta = 55^\circ$: \blacktriangle – $E = 50$ keV, \triangle – $E = 60$ keV; \bullet – $d = 633$ Å, $\theta = 30^\circ$, $E = 50$ keV. c – Ag, $d = 662$ Å, $E = 60$ keV, $\theta = 55^\circ$: \triangle – $\sim 1/E$ component, \blacktriangle – $\sim E^2$ component; curve 1 – theoretical for bremsstrahlung from [21], 2 – from [17] (enhanced 10 times).

perpendicular radiation component in the case of oblique electron incidence. The same components of the spectral distribution are shown in Fig. 8c; the total distributions for gold and silver foils are shown in Fig. 8a and Fig. 8b, respectively.

It follows from Fig. 8c that bremsstrahlung has a more pronounced spectral dependence than transition radiation. The experimental data in Fig. 9 show that the intensity of the perpendicular component for silver foils, measured for different observation angles and wavelengths, does not depend greatly on the thicknesses of the aforementioned films. The same pattern is observed for the $1/E$ and E^2 components (Fig. 9c).

It is seen on the whole from the data that the investigation of bremsstrahlung was hampered under our experimental conditions by the low intensity of the perpendicular component and by the

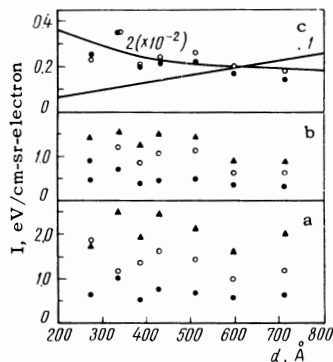


FIG. 9. Intensity of perpendicular component vs thickness of silver foils for $E = 50$ keV. a – $\theta = 25^\circ$, b – $\theta = 60^\circ$: \bullet – $\lambda = 4760$ Å, \circ – $\lambda = 4000$ Å, \blacktriangle – $\lambda = 3480$ Å; c – $\lambda = 4670$ Å, $\theta = 50^\circ$: \circ – $\sim 1/E$ component; \bullet – $\sim E^2$ component; 1 – theory of bremsstrahlung from [21], 2 – from [17] (enhanced 100 times).

large contribution of the transition radiation. It was therefore shown by the investigation of optical frequencies observed when nonrelativistic electrons pass through thin metal foils that this emission is mainly transition radiation, and that its intensity depends essentially on the optical constants of the metals. In the cases of silver and gold foils bremsstrahlung was also identified, with about one-tenth the intensity of the transition radiation.

c) Polarization of transition radiation. This is one of the principal features of transition radiation. Its complete polarization is often utilized to discriminate it from other types of radiation. It has been shown by Pafomov [24] that elliptically polarized radiation should be observed when a charged particle crosses obliquely the interface between two media having different optical properties. When a particle impinges normally on the surface of an optically isotropic medium the electric vector of the radiation lies in the plane passing through the line of sight and the direction of particle motion. We shall now discuss some of the polarization properties of light observed in connection with normally and obliquely impinging electrons.

The radiation intensity was measured as a function of the angle φ between the transmission plane of the polarizing filter and the plane containing the normal to the foil surface and the direction of observation ($\varphi = 0$). We investigated the dependence of the degree of polarization

$$P = (I_{\parallel} - I_{\perp}) / (I_{\parallel} + I_{\perp}) \quad (1)$$

on the experimental conditions; where I_{\parallel} and I_{\perp} are the light intensities at $\varphi = 0$ and 90° , respectively.

The experimental results (Fig. 10) as a whole reveal the dependence $A + B \cos^2 \varphi$. The data for different materials, the observation angles θ (measured from the initial direction of electron motion), electron energies and wavelengths for normal electron incidence ($\psi = 0^\circ$) show that the radiation is polarized in the plane $\varphi = 0^\circ$.

Figure 10c shows the dependence of the intensity on φ for oblique electron incidence on the aluminum foil surface at different incident angles ψ (the angle between the normal to the foil surface and the direction of electron motion). While no perpendicular component is observed for $\psi = 0^\circ$, when ψ differs from zero its intensity increases appreciably and continues to grow with ψ . The maximum intensity is no longer observed at $\varphi = 0^\circ$, as with normal electron incidence. The deviation of the maximum increases with ψ and reaches $\varphi = 14^\circ \pm 5^\circ$ at $\psi = 30^\circ$. It is seen from the same figure that for fixed ψ this deviation is independent of the electron energy.

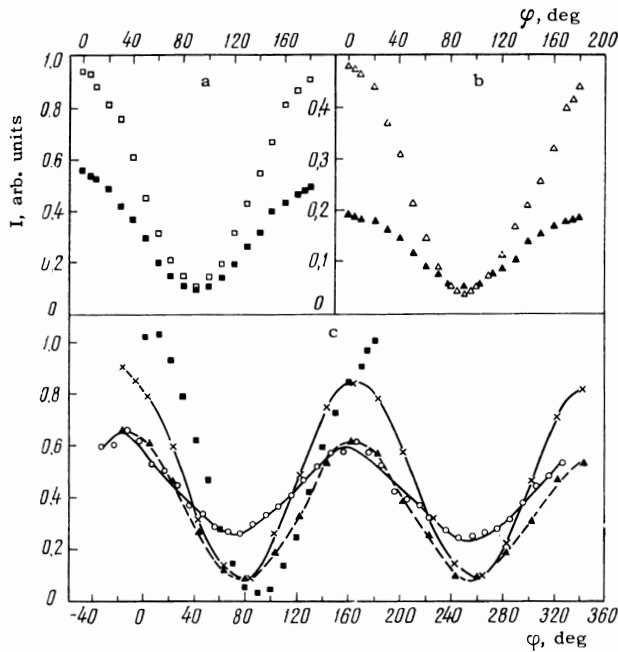


FIG. 10. Radiation intensity vs the angle φ . a - Ag, $\psi = 0^\circ$, $\lambda = 4670 \text{ \AA}$, $d = 767 \text{ \AA}$, $\theta = 60^\circ$: \square - $E = 50 \text{ keV}$, \blacksquare - $E = 30 \text{ keV}$. b - Au, $\psi = 0^\circ$, $\lambda = 3820 \text{ \AA}$, $d = 361 \text{ \AA}$, $E = 60 \text{ keV}$: \triangle - $\theta = 50^\circ$, \blacktriangle - $\theta = 20^\circ$. c - Al, \blacksquare - $\psi = 0^\circ$, $\lambda = 4670 \text{ \AA}$, $d = 329 \text{ \AA}$, $E = 60 \text{ keV}$, $\theta = 50^\circ$; $\lambda = 4950 \text{ \AA}$, $\theta = 60^\circ$, $d = 209 \text{ \AA}$: \times - $\psi = 15^\circ$, $E = 60 \text{ keV}$; \blacktriangle - $\psi = 15^\circ$, $E = 40 \text{ keV}$; \circ - $\psi = 30^\circ$, $E = 60 \text{ keV}$.

With normal incidence of electrons on foils of different metals a high degree of polarization is observed independently of the emitted wavelength in the range 3480–5500 \AA (Fig. 11a). Within experimental error limits this degree of polarization is also independent of foil thickness. The data for silver foils with thicknesses from 273 to 976 \AA at $\psi = 0^\circ$ are shown in Fig. 11b. At $\theta = 25^\circ$ a relatively smaller value of P is observed, because the transition radiation intensity I_{\parallel} decreases at small angles, whereas I_{\perp} is relatively increased. A

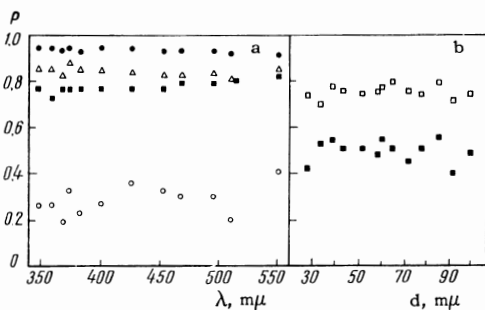


FIG. 11. Dependence of P on (a) emitted wavelength and (b) foil thickness. a - $\psi = 0^\circ$, $E = 60 \text{ keV}$: \bullet - Al, $d = 275 \text{ \AA}$, $\theta = 60^\circ$; \triangle - Au, $d = 327 \text{ \AA}$, $\theta = 50^\circ$; \blacksquare - Ag, $d = 662 \text{ \AA}$, $\theta = 55^\circ$; \circ - Al, $\psi = 30^\circ$, $E = 60 \text{ keV}$, $d = 252 \text{ \AA}$, $\theta = 50^\circ$. b - Ag, $\psi = 0^\circ$, $\lambda = 4000 \text{ \AA}$, $E = 50 \text{ keV}$: \square - $\theta = 50^\circ$; \blacksquare - $\theta = 25^\circ$.

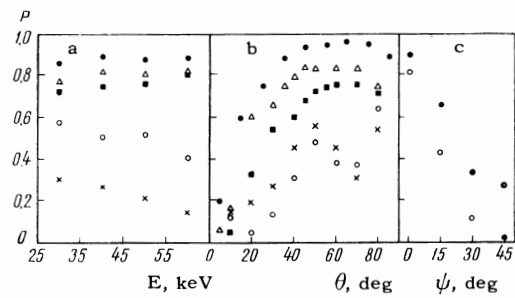


FIG. 12. Dependence of P on (a) electron energy, (b) angle of observation, and (c) angle of incidence ψ . a - $\psi = 0^\circ$, $\lambda = 4670 \text{ \AA}$, $\theta = 60^\circ$: \bullet - Al, $d = 133 \text{ \AA}$; \triangle - Au, $d = 361 \text{ \AA}$; \blacksquare - Ag, $d = 334 \text{ \AA}$. Al, $\psi = 30^\circ$, $\lambda = 4950 \text{ \AA}$, $d = 208 \text{ \AA}$: \circ - $\theta = 50^\circ$; \times - $\theta = 30^\circ$. b - $\psi = 0^\circ$: \bullet - Al, $\lambda = 4670 \text{ \AA}$, $d = 329 \text{ \AA}$, $E = 60 \text{ keV}$; \triangle - Au, $\lambda = 3820 \text{ \AA}$, $d = 361 \text{ \AA}$, $E = 60 \text{ keV}$; \blacksquare - Ag, $\lambda = 4670 \text{ \AA}$, $d = 666 \text{ \AA}$, $E = 50 \text{ keV}$. Al, $\psi = 30^\circ$, $\lambda = 4670 \text{ \AA}$, $d = 329 \text{ \AA}$: \times - $E = 60 \text{ keV}$; \circ - $E = 40 \text{ keV}$. c - Al, $\psi = 30^\circ$, $\lambda = 4670 \text{ \AA}$, $d = 127 \text{ \AA}$, $E = 60 \text{ keV}$: \bullet - $\theta = 60^\circ$; \circ - $\theta = 30^\circ$.

clearer illustration appears in Fig. 12b, which shows the dependence of P on the observation angle at small angles. P remains almost constant above $\theta = 45^\circ$. A certain increase of P with electron energy at $\psi = 0^\circ$ can be attributed to an increased yield of the transition radiation. At the same time I_{\perp} is either almost independent of electron energy or falls off slightly as the latter increases.

All the dependences of P (Figs. 11 and 12) for ψ differing from zero exhibit an appreciable variation of I_{\parallel} and I_{\perp} relative to each other. It should be noted that we did not analyze the light with a quarter-wave plate to determine the polarization, as is required for oblique electron incidence on a foil, which should then result in elliptically or circularly polarized light. In this case the radiation can be completely polarized even if P as previously defined equals zero (circular polarization). Therefore the data presented in Figs. 11 and 12 for ψ with nonzero experimental values are to be considered only with regard to the ratio of I_{\parallel} and I_{\perp} and their dependence on the experimental conditions. These dependences are compared with analogous calculations based on transition radiation equations for oblique passage of electrons through a foil.^[23] For example, the theory predicts the dependence

$$P = (1 - aE) / (1 + aE) \quad (2)$$

in which I_{\parallel} is proportional to E and I_{\perp} is proportional to E^2 . The corresponding experimental results shown in Fig. 12a agree well with the theory.

A similar analysis of experimental results with regard to their dependence on λ , θ , and ψ shows good agreement with experiment. P is below the predicted value, because the observed absolute

values of I_{\perp} are several times higher than the theoretical values.

For nonzero values of ψ the observed emission has thus been seen to agree with the theory of transition radiation. The I_{\perp} component is observed to increase with ψ , sometimes reaching the value of I_{\parallel} ; the former is absent in the case of normal incidence ($\psi = 0$). These observations indicate that the oblique passage of electrons through thin aluminum foils produces radiation with polarization properties that do not conflict with the theoretical elliptical polarization of transition radiation under the same conditions.

¹I. M. Frank and V. L. Ginzburg, *J. Phys. (USSR)* **9**, 353 (1945).

²V. L. Ginzburg and I. M. Frank, *JETP* **16**, 15 (1946).

³I. M. Frank, *UFN* **68**, 337 (1959) (Nobel Lecture) *Science* **131**, 702 (1960).

⁴I. M. Frank, *UFN* **75**, 231 (1961), *Soviet Phys. Uspekhi* **4**, 740 (1962).

⁵F. G. Bass and V. M. Yakovenko, *UFN* **86**, 189 (1965), *Soviet Phys. Uspekhi* **8**, 420 (1965).

⁶I. M. Frank, *UFN* **87**, 189 (1965), *Soviet Phys. Uspekhi* **8**, 729 (1966).

⁷V. E. Pafomov, *JETP* **33**, 1074 (1957), *Soviet Phys. JETP* **6**, 829 (1958).

⁸G. M. Garibyan and G. A. Chalikyan, *JETP* **35**, 1282 (1958), *Soviet Phys. JETP* **8**, 894 (1959).

⁹V. P. Silin and E. N. Fetisov, *JETP* **45**, 1572 (1963), *Soviet Phys. JETP* **18**, 1081 (1964).

¹⁰R. H. Ritchie and H. B. Eldridge, *Phys. Rev.* **126**, 1935 (1962).

¹¹B. W. Hakki and H. I. Krumme, *Proc. IRE* **49**, 1334 (1961).

¹²F. R. Arutyunyan, K. A. Ispiryan, and A. G.

Oganesyan, *YaF* **1**, 842 (1965), *Soviet JNP* **1**, 604 (1965).

¹³P. Goldsmith and J. V. Jelley, *Phil. Mag.* **4**, 836 (1959).

¹⁴S. Mikhalyak, Dissertation, Moscow State University, 1961.

¹⁵H. Boersch, C. Radloff, and G. Sauerbrey, *Z. Phys.* **165**, 464 (1961); H. Boersch, P. Dobberstein, D. Fritzsche, and G. Sauerbrey, *Z. Phys.* **187**, 97 (1965).

¹⁶A. L. Frank, E. T. Arakawa, and R. D. Birkhoff, *Phys. Rev.* **126**, 1947 (1962); E. T. Arakawa, L. C. Emerson, D. C. Hammer, and R. D. Birkhoff, *Phys. Rev.* **131**, 719 (1963).

¹⁷L. C. Emerson, E. T. Arakawa, R. H. Ritchie, and R. D. Birkhoff, *Emission Spectra of Electron Irradiated Metal Foils*, ORNL-3450, 1963.

¹⁸S. Tanaka and Y. Katayama, *J. Phys. Soc. Japan* **19**, 40 (1964).

¹⁹F. R. Arutyunyan, Zh. V. Petrosyan, and R. A. Oganesyan, *JETP Letters*, **3**, 193 (1966), transl. p. 123.

²⁰F. R. Arutyunyan, Zh. V. Petrosyan, and R. A. Oganesyan, *Opt. i Spektroskopiya* **9**, (1966).

²¹R. L. Gluckstern and M. H. Hull, *Phys. Rev.* **90**, 1030 (1953); R. L. Gluckstern, M. H. Hull, and G. Breit, *Phys. Rev.* **90**, 1026 (1953).

²²E. A. Taft and H. R. Philipp, *Phys. Rev.* **121**, 1100 (1961).

²³V. A. Engibaryan and G. V. Khachatryan, *Izv. AN Armenian SSR, Physics*, **1**, 2 (1966).

²⁴V. E. Pafomov, *On the Polarization of Transition Radiation*, *Phys. Inst. AN USSR, Preprint A-72*, 1964.

Translated by I. Emin